Supplementary Information

(1) XRD patterns of the RGD-PAA-UGNP powder sample before and after TGA

The as-prepared RGD-PAA-UGNP sample was amorphous owing to ultrasmall particle diameter,[1] whereas after TGA up to 900 ºC, sharp peaks were observed. All peaks after TGA could be assigned with (hkl) Miller indices and only the strong peaks were assigned in Fig. S1. The nanoparticles after TGA exhibited a cubic structure of Gd_2O_3 with cell constant of a = 10.82 Å owing to particle size growth and crystallization,[2] which is consistent with reported value (JCPDS card No. 43-1014).[3]
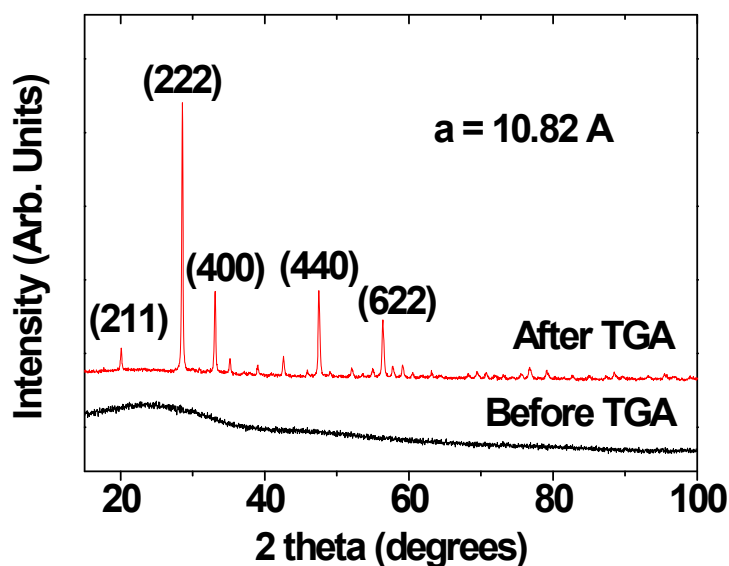

Fig. S1 XRD patterns of the RGD-PAA-UGNP powder sample before (bottom) and after (top) TGA. Only the strong peaks (i.e., the top XRD pattern) were assigned with (hkl) Miller indices, showing a cubic structure of Gd_2O_3.

(2) Surface-coating amount analysis

The surface-coating amount of the UGNPs with RGD-PAA was estimated to be 46.6% in wt.% from a TGA curve (Fig. S2). The initial drop (i.e., 11.7%) was due to water and air desorption. The remaining 41.7% was due to the UGNPs.
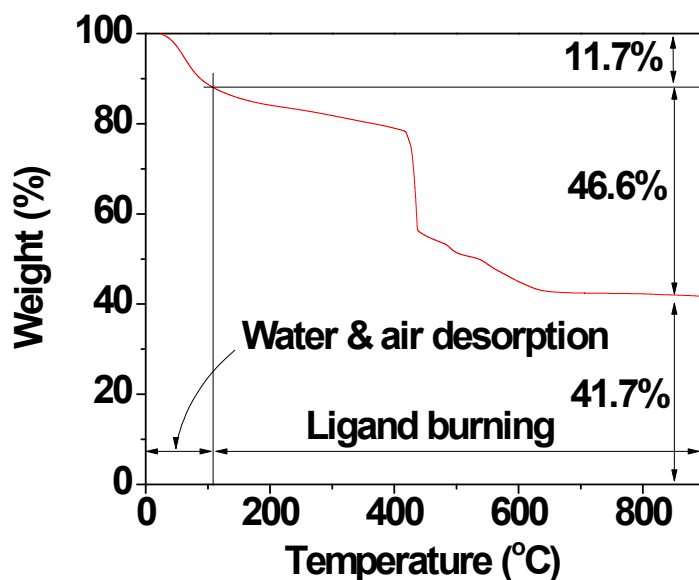

Fig. S2 TGA curve of the RGD-PAA-UGNP powder sample.

Grafting density,[4] corresponding to the average number of ligands coated per nanoparticle unit surface area, was estimated to be 0.82 nm^{-2} using the bulk density of Gd_2O_3 (7.41 g/cm^3),[5] the surface-coating amount of 46.6% estimated from TGA, the d_{avg} of 1.8 nm determined from HRTEM imaging, and the ligand mass of PAA (because the surface-coating ligand mass was mostly PAA). The number of PAAs coated per nanoparticle was estimated to be 8 or 9 by multiplying the grafting density by the nanoparticle surface area (πd^2_{avg}).

Considering the numbers of moles of Gd-precursor (2.0 mmol) and RGD (0.029 mmol) used in the synthesis, three or four RGDs were conjugated to each PAA-UGNP. To this calculation, the number of moles of PAA-UGNPs used for the synthesis of RGD-PAA-

UGNPs was calculated as follows. Because three-quarters of the synthesized PAA-UGNPs were used for the synthesis of RGD-PAA-UGNPs, $2.0 \times (3/4) = 1.5$ mmol of Gd were allocated to PAA-UGNPs for the synthesis of RGD-PAA-UGNPs. The number of Gd per UGNP was then estimated to be ~175 using a simple formula,[6] $N_{metal} \approx (x/y)(d_{avg}/h)^3$, where x = number of Gd^{3+} ions per chemical formula (= 2), y = number of all the ions per chemical formula (= 5), and h = average ionic diameter of all the ions[7] in the chemical formula (0.2372 nm for Gd_2O_3). From this, the number of moles of PAA-UGNPs was estimated to be $1.5/175 = 0.008571$. Therefore, RGD : PAA-UGNP = $0.029 : 0.008571 = 3.4 : 1$, which means that 3 or 4 RGDs were conjugated to each PAA-UGNP.

Using the above estimations, i.e., 8 or 9 PAAs and 3 or 4 RGDs per RGD-PAA-UGNP, and the chemical formulas of $C_{12}H_{22}N_6O_6$ (RGD) and $(C_3H_4O_2)_{n=25}$ (PAA), the C/H/O/N mole ratios in the RGD-PAA-UGNP were estimated to be 35.3/48.1/23.2/1.0 for PAA = 8 and RGD = 3, 27.0/37.0/17.7/1.0 for PAA = 8 and RGD = 4, 39.5/53.7/26.0/1.0 for PAA = 9 and RGD = 3, and 30.1/41.2/19.8/1.0 for PAA = 9 and RGD = 4. These results are fairly consistent with 27.08/51.10/19.37/1.00 estimated from EA data (see text). Therefore, the above-estimated numbers of PAAs and RGDs per RGD-PAA-UGNP seem to be reasonable.

(3) Water proton relaxivities

The r_1 and r_2 values of the RGD-PAA-UGNPs in aqueous solution were estimated to be 13.28 ± 0.07 and 15.51 ± 0.71 $s^{-1}mM^{-1}$, respectively, from the $1/T_1$ and $1/T_2$ plots versus the Gd concentration (Fig. S3). As a reference, a commercial molecular agent Gadovist was also measured ($r_1 = 4.40 \pm 0.10$; $r_2 = 4.72 \pm 0.09$ $s^{-1}mM^{-1}$)[8] (Fig. S3). r_1 and r_2 values of the sample solution were approximately 3 times higher than those of the Gadovist, indicating that the

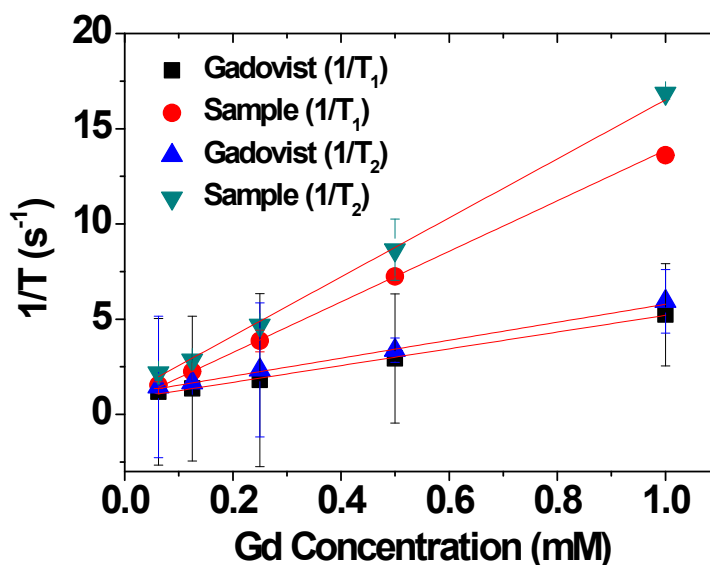solution sample is more powerful than the Gadovist in T_1 MRI.

Fig. S3 Plots of $1/T_1$ and $1/T_2$ versus Gd concentration. The slopes of $1/T_1$ and $1/T_2$ correspond to r_1 and r_2 values, respectively.

(4) Photographs and T_1 MR images of the four mice groups before and after thermal neutron beam irradiation

Both photographs and T_1 MR images taken before and day 23 or 24 or 25 after thermal neutron irradiation are provided in Fig. S4, showing that the cancer volume growth is in the order of Gd-/n- > Gd+/n- > Gd-/n+ > Gd+/n+. The mice used for photographing are not necessarily the same as those used for MRI, but they belong to the same mice group.

4

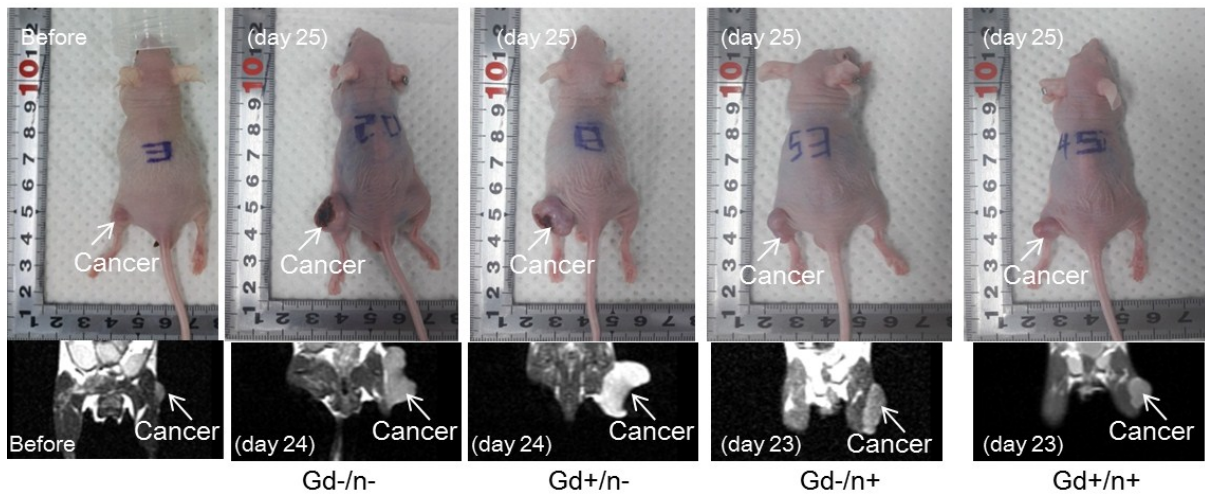Photographs (top) and T$_1$ MR images (bottom)

Fig. S4 Photographs (top) and T$_1$ MR images (bottom) of the four mice groups before and day 23 or 24 or 25 after thermal neutron beam irradiation.

(5) The GdNCT experimental facilities and teflon shielding for GdNCT experiment

The GdNCT experiments were conducted using the cyclotron (MC50, Scanditronix, Sweden) and beam irradiation facilities installed at the Korea Institute of Radiological & Medical Science (Fig. S5). The cyclotron was operated at 35 MeV and 20 μA with ^{9}Be target (diameter = 17 mm) to generate thermal neutron beam. The generated thermal neutron beam dose was set as 1.0 Gy/12 min.

Only the cancer site of the mice was exposed to the thermal neutron beam and the other parts of the mice were shielded using a thick teflon plate (Fig. S6) to protect them from damage by thermal neutron beam.

Fig. S5 The MC50 cyclotron (left) and thermal neutron beam irradiation (right) facilities at the Korea Institute of Radiological & Medical Science.

Fig. S6 Teflon shielding used to protect the mice from thermal neutron beam irradiation.

References

1 F. Söderlind, H. Pedersen, R. M. Petoral, P. O. Käll and Uvdal, *J. Colloid Interface Sci.*, 2005, **288**, 140-148.

2 K. Kattel, J. Y. Park, W. Xu, H. G. Kim, E. J. Lee, B. A. Bony, W. C. Heo, J. J. Lee, S. Jin,

J. S. Baeck, Y. Chang, T. J. Kim, J. E. Bae, K. S. Chae and G. H. Lee, *ACS Appl. Mater. Interfaces*, 2011, **3**, 3325-3334.

3 *JCPDS-International Centre for Diffraction Data*, card no. 43-1014, PCPDFWIN, vol. 1.30, 1997.

4 M. K. Corbierre, N. S. Cameron and R. B. Lennox, *Langmuir*, 2004, **20**, 2867-2873.

5 W. M. Haynes, D. R. Lide and T. J. Bruno, *CRC Handbook of Chemistry and Physics*, 96th Edition, CRC Press, Boca Raton, USA, 2015-2016, p. 4-64.

6 S. J. Kim, W. Xu, M. W. Ahmad, J. S. Baeck, Y. Chang, J. E. Bae, K. S. Chae, T. J. Kim, J. A. Park and G. H. Lee, *Sci. Technol. Adv. Mater.*, 2015, **16**, 055003 (9pp).

7 R. D. Shannon, *Acta Cryst.*, 1976, A**32**, 751- 767.

8 Gadobutrol, Bayer Scherring Pharma, Germany.